Mitogen-activated protein kinase-activated protein kinase 2 mediates resistance to Hydrogen peroxide-induced oxidative stress in Human hepatobiliary Cancer cells

Thang Huong Nguyen Ho-Bouldoires, Audrey Clapéron, Martine Mergey, Dominique Wendum, Christèle Desbois-Mouthon, Sylvana Tahraoui, Laetitia Fartoux, Hamza Chettouh, Fatiha Merabtene, Olivier Scatton, et al.

HAL Id: hal-01176572

https://hal.sorbonne-universite.fr/hal-01176572v1

Submitted on 15 Jul 2015

Mitogen-activated protein kinase-activated protein kinase 2 mediates resistance to hydrogen peroxide-induced oxidative stress in human hepatobiliary cancer cells

Thanh Huong Nguyen Ho-Bouldoires[1,2], Audrey Clapéron[1,2], Martine Mergey[1,2], Dominique Wendum[1,2,3], Christèle Desbois-Mouthon[1,2], Sylvana Tahraoui[1,2], Laetitia Fartoux[1,2,4], Hamza Chettouh[1,2], Fatiha Merabtene[1,2], Olivier Scatton[1,2,5], Matthias Gaestel[6], Françoise Praz[1,2], Chantal Housset[1,2,4], and Laura Fouassier[1,2]

[1]INSERM, UMR_S 938, Centre de Recherche Saint-Antoine, F-75012, Paris, France;

[2]Sorbonne Universités, UPMC Univ Paris 06, UMR_S 938, Centre de Recherche Saint-Antoine, F-75012, Paris, France;

[3]AP-HP, Hôpital Saint-Antoine, Service d'Anatomie et Cytologie Pathologiques, F-75012 Paris, France;

[4]AP-HP, Hôpital Saint-Antoine, Service d'Hépatologie, F-75012 Paris, France;

[5]AP-HP, Hôpital Saint-Antoine, Service de Chirurgie Hépato-Biliaire et Transplantation Hépatique, F-75012, Paris, France;

[6]Institute of Physiological Chemistry, Hannover Medical School, Carl-Neuberg-Str. 1, D-30625 Hannover, Germany

*Running title: MK2-mediated resistance to oxidative stress in liver cancer

To whom correspondence should be addressed:

Laura Fouassier, Ph.D.

INSERM UMR_S938, Centre de Recherche Saint-Antoine

MK2-mediated resistance to oxidative stress in liver cancer

184 rue du Faubourg Saint-Antoine

75571 - Paris cedex 12, France

Tel: (33) 6 98 77 40 01

E-mail: laura.fouassier@inserm.fr

Abstract

The development and progression of liver cancer are characterized by increased levels of reactive oxygen species (ROS). ROS-induced oxidative stress impairs cell proliferation and ultimately leads to cell death. Although liver cancer cells are especially resistant to oxidative stress, mechanisms of such resistance remain understudied. We identified the MAPK-activated protein kinase 2 (MK2)/Heat shock protein 27 (Hsp27) signaling pathway mediating defenses against oxidative stress. Besides to MK2 and Hsp27 overexpression in primary liver tumors compared to adjacent non-tumorous tissues, MK2/Hsp27 pathway is activated by hydrogen peroxide-induced oxidative stress in hepatobiliary cancer cells. MK2 inactivation or inhibition of MK2 or Hsp27 expression increases Caspase-3 and PARP cleavage and DNA breaks, and therefore cell death. Interestingly, MK2/Hsp27 inhibition decreases antioxidant defenses such as heme-oxygenase 1 (HO-1) through down-regulation of the transcription factor nuclear factor-erythroid-derived 2-like 2 (Nrf2). Moreover, MK2/Hsp27 inhibition decreases both phosphorylation of epidermal growth factor receptor (EGFR) and expression of its ligand, heparin-binding EGF-like growth factor (HB-EGF). A new identified partner of MK2, the scaffold PDZ-protein EBP50, could facilitate these effects through MK2/Hsp27 pathway regulation. These findings demonstrate that MK2/Hsp27 pathway actively participates in resistance to oxidative stress and may contribute to liver cancer progression.

3

Introduction

The development of primary malignant tumors of the liver, hepatocellular carcinoma (HCC) and cholangiocarcinoma (CCA), is associated with chronic viral infections (*i.e.* viral hepatitis B or C), excessive alcohol consumption or metabolic diseases [1, 2]. All these conditions contribute to reactive oxygen species (ROS) production leading to oxidative stress in the course of liver carcinogenesis [3-8]. ROS content was previously found to be higher in human HCC biopsies than in chronic viral infection biopsies indicating that ROS may play a role in tumor promotion and progression [9].

In fact, ROS accumulation triggers cell component oxidation and overwhelming damages usually drive to cell death. But resistance to oxidative stress can conduct to abnormal proliferation and transformation. Cancer cells developing adaptive abilities to oxidative environment ultimately promote tumor progression and chemoresistance [10]. Some of adaptive mechanisms depend on ROS-activated oncogenic signaling pathways essential for cell survival. Thus, H_2O_2 activates the mitogen-activated protein kinase (MAPK)-activated protein kinase 2 (MAPKAPK2 or MK2) [11-13], which belongs to the stress-activated p38 MAPK cascade [14, 15]. MK2 regulates pleiotropic cellular functions that have been previously well described including inflammatory response [16, 17], resistance to chemotherapy [18-20], and more recently resistance to oxidative stress [21, 22].

MK2 functions are mediated by the phosphorylation of several substrates. The heat shock protein Hsp27 is the *bona fide* substrate of MK2 [16, 23]. Hsp27 displays anti-apoptotic properties [24, 25] and regulates the expression of proinflammatory chemokines involved in cancer cell survival [26, 27]. MK2 can also phosphorylate the pro-survival kinase Akt [28], Mouse Double Minute 2 homolog (MDM2) [29], a negative regulator of the pro-apoptotic

protein p53. Overexpression of MK2 has been demonstrated in multiple myeloma [30], lung cancer [31], gastrointestinal stromal tumors [32] and breast cancer [33].

Although ROS-induced oxidative stress is omnipresent during liver carcinogenesis and progression, MK2 status, function and regulation in liver cancer remain unknown. We aim to decipher the role of MK2 in human liver cancer cell response to oxidative stress. Here, we show that MK2 mediates resistance to oxidative stress in liver cancer cells by stimulating survival signals through both activation of antioxidant defenses and HB-EGF/EGFR axis. Additionally, we identify a new MK2 binding protein, the scaffold protein EBP50 as a regulator of the MK2-dependent pathway during oxidative stress. Overall, the present work highlights the involvement of MK2 pathway in the adaptation to oxidative stress that may participate to liver carcinogenesis.

Materials and methods

Patients and liver tumor specimens

Samples of HCC and paired adjacent nontumoral liver tissue (n = 70 pairs) or intrahepatic CCA tumors (n = 10) were obtained from patients who underwent liver resection in Saint-Antoine Hospital (AP-HP, Tumor bank HUEP, "Tumeur Est") in accordance with the French laws and regulations (CNIL, registration N° ckT0915543z). Characteristics of patients with HCC and CCA are provided in Table 1. Adjacent non tumoral liver tissue of patients with CCA showed no significant fibrosis except in one patient who had chronic hepatitis B with few fibrous septa. Histologically normal liver tissue (control liver samples) was obtained from 8 patients who underwent partial hepatectomy for the treatment of metastases or benign tumor. Tissue samples were snap-frozen in liquid nitrogen and stored at -80°C until analysis.

Immunostaining

For immunohistochemistry, paraffin-embedded human liver tissue samples were cut in 4-µm sections and antigens were unmasked as indicated in Table 2. Sections were incubated sequentially with H_2O_2 for 5 min, with blocking serum (Protein block serum-free, Dako, Les Ulis, France) for 20 min, with primary antibodies (Table 2) for 30 min and with secondary biotinylated antibodies (Trekkie Biotinylated Rabbit/Mouse link, Biocare Medical, Les Ulis, France) for 20 min. Sections were finally incubated with TrekAvidin-HRP for 20 min. The Autostainer Plus (Dako) was used to perform immunostaining. The color was developed using amino-ethyl-carbazole (AEC peroxidase substrate kit; Vector Laboratories, Les Ulis, France). Sections were counterstained with haematoxylin and mounted with glycergel (Dako).

For immunofluorescence, cells were fixed in 4% paraformaldehyde for 15 min, permeabilized in 0.1% Surfact-Amps X100 (Thermo Scientific, Courtaboeuf, France) and blocked with 1% albumin and 10% goat serum for 1 h at room temperature. Cells were incubated overnight with

primary antibodies (Table 2) and then for 1 h at room temperature with secondary fluorescent antibodies (Invitrogen, Saint Aubin, France). Cell nuclei were counterstained with DRAG-5 (Invitrogen) for 5 min during the final wash before mounting (Fluoromount; EMS, France). Cells were observed with an epifluorescence or an SP2 confocal microscope (Leica, Nanterre, France).

Cell models

Human HCC cell lines included PLC/PRF/5 cells provided by Dr. C. Perret (Institut Cochin, Paris, France), and HepG2 cells from ATCC. Human CCA cell lines included Mz-ChA-1 cells provided by Dr. A. Knuth (Zurich University, Switzerland) and TFK1 cells obtained from DSMZ, Germany. HeLa cells were obtained from ATCC.

Cells were incubated with hydrogen peroxide (H_2O_2) from Sigma-Aldrich to induce oxidative stress. In experiments, the MK2 inhibitor (MK2 inhibitor III, Merck, Millipore, Guyancourt, France) (5 μM) was added to the culture medium 1 h before treatment with H_2O_2.

Cell viability

Cell viability was measured using the 3-(4,5-dimethylthiazol-2-yl)-2,5-diphenyltetrazolium bromide (MTT) assay. Cells were incubated with MTT dye at the final concentration of 0.1 mg/mL for 4h at 37°C. Absorbance was quantified by a spectrophotometer (Tecan, Lyon, France) at 560 nm.

RNA silencing

MK2, Hsp27, Nrf2 and EBP50 expression was silenced by using a pool of four small interfering RNA (siRNA) (ON-TARGET*plus* SMARTpool, Dharmacon). Control siRNA was a pool from Dharmacon (siGENOME non-targeting siRNA pool 2). Transient transfections were performed with 75-100 nM of siRNA using DharmaFECT 4 (Thermo Scientific).

RNA isolation and gene expression analysis

Total RNA was extracted from cell cultures using RNeasy Mini Kit (Qiagen, Courtaboeuf, France). For tissues, a preliminary RNA extraction step was conducted using TRIzol Reagent (Life Technologies). RNA was reverse-transcribed and quantified by real time PCR on a LightCycler® 480 instrument (Roche Diagnostics) using SYBR Green chemistry and specific primers (Table 3). For each sample, gene expression was normalized to hypoxanthine phosphoribosyltransferase (*HPRT*) mRNA content and was expressed relatively to the same calibrator (for human samples). The relative quantity of each target mRNA was determined from duplicates using the formula $2^{-\Delta\Delta CT}$.

Immunoprecipitation and western blot analysis

For immunoprecipitation, cells were harvested in the immunoprecipitation buffer containing NP-40 (1 %) supplemented with 1 mM orthovanadate and a protease inhibitor cocktail (Roche Diagnostics) and subjected to centrifugation for 15 min at 4 °C at 21 000 g. Precleared proteins (1 mg) were incubated with antibodies (4 μg) (Table 2) overnight at 4 °C. Proteins immunoprecipitated from protein A/G sepharose beads were suspended in Laëmmli buffer (Bio-Rad, Marnes-La-Coquette, France) and subjected to western blot analysis.

For western blot analysis, cells were lysed on ice directly in Laëmmli buffer supplemented withþβ-mercaptoethanol for short time stimulations or in RIPA buffer supplemented with 1 mM orthovanadate and a cocktail of protease inhibitors for treatments of 6-24 hours. In condition of lysis in RIPA, proteins were quantified using a BCA kit (Pierce). Proteins were heated for 5 min at 95°C, subjected to SDS-PAGE migration and transferred to nitrocellulose membranes (Bio-Rad). The blots were blocked with TBS 0.1 % Tween-20 containing 5% bovine serum albumin and incubated with primary antibodies (Table 2) overnight at 4°C and with secondary horseradish peroxidase-linked antibodies (Cell Signaling) for 1 h at room temperature. Immune

complexes were visualized by enhanced chemiluminescence (Pierce, Courtaboeuf, France). Band signal quantification was achieved using ImageJ.

Measurement of ROS Production

ROS production was evaluated using dihydroethidium fluorescent probe (DHE, Sigma, L'Isle d'Abeau Chesnes, France). Briefly, treated-cells were incubated with 50 mM DHE fluorescent probe at 37°C for 30 min and then extensively washed with PBS to remove the residual probe. The fluorescence intensity was measured at 510 nm (excitation wavelength) and 605 nm (emission wavelength) using a luminometer (Tecan, Lyon, France). Measurement was reported on the protein content per well.

Yeast two-hybrid (Y2H) screen

The coding sequence of human EBP50 (GI number 29165827) was amplified by PCR and cloned into pENTR™/D-TOPO® (Invitrogen). Bait cloning into pB27 (N-LexA-bait C fusion) and Y2H screening of a commercialized human liver cDNA library (human liver RP1) were performed by Hybrigenics, Paris, France. Eighty-two millions interactions were tested with EBP50 and after selection, 272 positive clones were analyzed. cDNA fragments corresponding to positive "prey" clones were amplified by PCR and sequenced at their 5′ and 3′ junctions. The resulting sequences were searched against GenBank using a fully automated procedure, assigned a "Predicted Biological Score" indicative of the interaction confidence.

Glutathione-S-transferase (GST) pull-down

GST pull-down was performed as previously described [34]. Protein lysates from HeLa cells were incubated with GST-fusion protein beads for 2 h at 4°C. The beads were extensively washed with PBS. Bound protein fractions were eluted with Laëmmli buffer and analyzed by western blot.

Statistical analysis

9

Results are given as mean ± SEM. Data were analyzed using Prism 5.0 software (GraphPad Software Inc.). Data obtained from *in vitro* experiments with cell lines were analyzed using Student's t-test, Wilcoxon signed-rank test or Mann-Whitney U-test. Tests were two-sided. Expression data obtained from human tissue specimens were analyzed using Mann-Whitney U test (unpaired data) and Wilcoxon test (paired data). Correlations between MK2 and Hsp27 or EBP50 mRNA expression and between Hsp27 and EBP50 mRNA expression in human liver tissue samples were conducted using Spearman rank correlation coefficient. *P* value of less than 0.05 was considered significant.

Results

MK2 and Hsp27 expression is upregulated in human liver tumors

We first analyzed whether MK2 and Hsp27 were expressed in human liver cancers. We examined the mRNA levels of MK2 and Hsp27 in 70 HCC tumors (T) and paired surrounding non-tumor liver tissues (NT), as well as in 8 healthy livers. MK2 and Hsp27 mRNA levels were similar between non-tumor and healthy liver tissues (data not shown), whereas they were significantly higher in HCC tumors compared with matched non-tumor tissues (Fig. 1A, left and middle panels). Spearman correlation analysis showed a strong correlation between the levels of both transcripts (r=0.59, p<0.0001). To validate these data at the protein level, immunohistochemistry of MK2 and Hsp27 was performed (Fig. 1B) on 7 HCC tumors. Both proteins were found highly expressed in tumor cells compared with matched non-tumor tissues. Immunohistochemistry analysis was also performed in 10 CCA tumors in which a higher expression of MK2 and Hsp27 was observed in comparison with adjacent non-malignant bile duct epithelium (Fig. 1C). These results suggest that MK2/Hsp27 signaling can operate in human liver cancers.

The MK2 pathway is activated by oxidative stress in liver cancer cells

It has been described that MK2 can be activated by oxidative stress, we thus analyzed MK2/Hsp27 pathway activation by exposing human liver cell lines, PLC/PRF/5 (HCC cells) and Mz-ChA-1 (CCA cells) to increasing doses of hydrogen peroxide (H_2O_2 0.05-1 mM) in serum-supplemented medium (Fig. S1). MK2 was visualized in western blot assays with a specific antibody that recognizes MK2 irrespective of its phosphorylation status; MK2 phosphorylation was detected by a shift of electrophoretic mobility. We noticed that MK2 was strongly phosphorylated between 0.25 and 1 mM of H_2O_2 along with the phosphorylation of its *bona fide*

substrate Hsp27 (Fig. S1). A time-course of the MK2/Hsp27 pathway activation was then determined (Fig. 2A). HCC (PLC/PRF/5, HepG2) and CCA (Mz-ChA-1, TFK-1) cells were exposed to an intermediate dose of H_2O_2 (0.5 mM) for 0.5, 1 and 2 h (Fig. 2A, left part of the panels). MK2 and Hsp27 were phosphorylated in a time-dependent manner in HepG2 and TFK-1 cells unlike in PLC/PRF/5 and Mz-ChA-1 where MK2 and Hsp27 phosphorylation had already reached a plateau at 0.5 h (Fig. 2A, left part of the panels). Differences in time-course between cell lines could be explained by levels of MK2/Hsp27 expression and/or endogenous antioxidant defense.

The kinase activity of MK2 was inhibited by selective chemical MK2 inhibitor III (MK2i). MK2i is an ATP-competitive inhibitor of MK2 that has been characterized previously [35]; it has no effect on p38-dependent MK2 activation but prevents the phosphorylation of its downstream substrates. MK2 inhibition markedly decreased the phosphorylation of Hsp27 in H_2O_2-exposed cells (Fig. 2A, right part of the panels). Similarly, downregulation of MK2 by siRNA in two cell lines representative of HCC and CCA, PLC/PRF/5 and Mz-Ch-A1 respectively, decreased H_2O_2-induced Hsp27 phosphorylation (Fig. 2B).

These results suggest that H_2O_2-induced oxidative stress in HCC and CCA cells activates MK2/Hsp27 signaling pathway.

MK2 inhibition decreases liver cancer cell ability to survive in oxidative environment

Oxidative environment can lead to proliferation slowdown or/and cell death. Therefore, we wondered whether MK2 could confer survival advantage to cells subjected to such environment. We analyzed survival of HCC and CCA cells treated with H_2O_2 (0.1-1 mM) with or without MK2 inhibition. In all cell lines (Fig. 2C and S2A), H_2O_2 at the concentrations of 0.25-1 mM

decreased cell viability in a dose-dependent way. MK2 inhibition combined to H_2O_2 treatment caused a higher reduction of cell viability than H_2O_2 or MK2i alone (Fig. 2C and S2A).

Next, we analyzed caspase-3 and poly(ADP-ribose) polymerase (PARP) cleavage to determine whether apoptosis could be a mechanism responsible for the observed decreased survival. When combined to H_2O_2, MK2i induced a stronger cleavage of caspase-3 and PARP compared to either treatment alone (Fig. 3A and S2B). Similar results were obtained after downregulation of MK2 (Fig. 3B) or Hsp27 (Fig. 3C) expression with siRNA in HCC and CCA cells. Apoptosis induced by MK2i in H_2O_2-treated cells correlated with an increase in DNA breaks. A greater increase in nuclear foci number (Fig. 4A and B) and total protein expression (Fig. 4C) of γH2AX, a marker of DNA double-strand breaks, were observed in condition of H_2O_2 and MK2i treatment compared to H_2O_2 or MK2i alone. Similar results on total protein expression of γH2AX were obtained when Hsp27 was down-regulated by siRNA in cells (Fig. 4D)

These findings indicate that MK2/Hsp27 pathway displays survival benefits to liver cancer cells in oxidative condition.

MK2 inhibition diminishes antioxidant defenses in liver cancer cells

To further understand by which mechanisms, MK2 allows liver cancer cell survival during oxidative stress, we examined antioxidant defenses. The nuclear factor-erythroid-derived 2-like 2 (Nrf2) is a major regulator of the antioxidant response. Nrf2 induces the transcription of genes encoding antioxidant proteins such as heme oxygenase 1 (HO-1) [36]. Upon exposure to H_2O_2, Nrf2 accumulated in the nucleus of HCC and CCA cells (Fig. 5A, upper part of the panels) followed by an increased expression of HO-1 in these cells (Fig. 5B). MK2 inhibition prevented Nrf2 nuclear translocation (Fig. 5A, lower part of the panels) and reduced HO-1 expression (Fig. 5B) induced by H_2O_2.

HO-1 regulation by Nrf2 was validated in cells in which Nrf2 was down-regulated by siRNA. While Nrf2 protein level increased upon H_2O_2, Nrf2 reduction by siRNA caused a marked decrease of HO-1 expression in H_2O_2-treated cells (Fig. 5C). This decrease occurred along with an increase in DNA breaks as attested by a higher γH2AX expression (Fig. 5D). Antioxidant response downregulation by MK2i resulted in a significant increase in ROS content detected by dihydroethidium (DHE) fluorescence in cells exposed to H_2O_2 for 24 h (Fig. 5E). Hsp27 also regulated Nrf2 and HO-1 expression. Inhibition of Hsp27 by siRNA diminished Nrf2 and HO-1 level in H_2O_2-treated cells (Fig. 5F) compared to H_2O_2 condition.

These data suggest that MK2/Hsp27 pathway counteracts oxidative stress through antioxidant response activation.

Inhibition of MK2 abrogates H_2O_2-induced HB-EGF/EGFR axis in liver cancer cells

It has been shown that H_2O_2 mediates EGFR phosphorylation and increases expression of EGFR ligands in epithelial cell types [37-39]. We thus investigated the involvement of MK2 pathway in this regulation. In liver cancer cells, H_2O_2 induced the phosphorylation of EGFR (Fig. 6A and B) and caused a twofold augmentation of HB-EGF mRNA (Fig. 6C and D) and amphiregulin expression (data not shown). Inhibition of MK2 by MK2i (Fig. 6A and C) or Hsp27 by siRNA (Fig. 6B and D) led to a significant reduction of H_2O_2-induced phosphorylation of EGFR (Fig. 6A and B) and expression of HB-EGF mRNA (Fig. 6C and D) but not amphiregulin mRNA (data not shown). MK2i decreased likewise HB-EGF protein content in H_2O_2-treated cells (Fig. 6E).

Furthermore, we demonstrated that HB-EGF stimulates MK2 allowing probably an autocrine loop of MK2 pathway activation. Exogenous HB-EGF addition to liver cancer cells caused an

activation of MK2 and a phosphorylation of Hsp27 (Fig. 6F). MK2 inhibition strongly decreased HB-EGF-induced Hsp27 phosphorylation but not MK2 phosphorylation (Fig. 6F).

These results suggest that MK2/Hsp27 pathway function can operate through a regulation of HB-EGF/EGFR signaling.

The MK2/Hsp27 signaling is regulated by the scaffold protein ezrin-radixin-moesin-binding phosphoprotein 50 (EBP50)

A yeast two-hybrid screen of human liver cDNA identified EBP50, a PDZ protein highly expressed in the liver, as a binding protein of MK2. Consistently, the analysis of the MK2 protein sequence revealed the presence of a PDZ motif (LTRL) at the C-terminus (Fig. 7A). The interaction between both proteins was confirmed by GST pull-down and by immunoprecipitation (Fig. 7B and C). GST pull-down experiments were performed with HeLa cell lysates using GST-EBP50 fusion proteins containing either EBP50 wt or each of both PDZ domains of EBP50, PDZ1 and PDZ2 (Fig. 7B). Western blot analysis indicated that MK2 binds both PDZ domains of EBP50. In this experiment, Akt, which is a binding partner for EBP50, was used as a positive control [40]. Reciprocal immunoprecipitation experiments using either MK2 (Fig. 7C, left panel) or EBP50 antibody (Fig. 7C, right panel) showed that EBP50 interacted with MK2 and phospho-MK2 in Mz-ChA-1 cells.

We then analyzed whether EBP50 could modulate MK2-dependent signaling in cells subjected to oxidative stress. In HCC and CCA cell lines treated with H_2O_2, EBP50 downregulation with siRNA reduced Hsp27 phosphorylation (Fig. 7D). MK2 phosphorylation remained unaffected suggesting that EBP50 does not modulate the MK2 activation but rather scaffolds MK2 in close proximity to its substrates. This result indicates that EBP50 is required for Hsp27 phosphorylation in oxidative stress condition. Interestingly, GST pull-down analysis showed that

Hsp27 associated with EBP50 only when cells were treated with H_2O_2 and not in control conditions (Fig. 6E). Functionally, EBP50 downregulation by siRNA induced a higher increase in H_2O_2-induced caspase-3 and PARP cleavage (Fig. 7F) and DNA breaks attested by γH2AX protein expression (Fig. 7G), compared to H_2O_2 condition.

Finally, we examined the EBP50 mRNA level in HCC tumors (T) and paired surrounding non-tumor liver tissues (NT) as well as in 8 healthy livers. EBP50 mRNA level was similar between non-tumor liver tissues and healthy livers (data not shown), whereas it was significantly higher in HCC tumors compared with matched non-tumor tissues (Fig. 8A). Spearman correlation analysis showed a strong correlation between EBP50 and MK2 mRNA (r=0,64, p<0.0001) and between EBP50 and Hsp27 mRNA (r=0.60, p<0.0001) (Fig. 8B). We next investigated EBP50 protein expression by immunohistochemistry on 7 HCC and 10 CCA tumors. The protein was found highly expressed in tumor cells compared with matched non-tumor tissues in HCC (Fig. 8C left panel), and in CCA compared to adjacent non-malignant bile duct epithelium (Fig. 8C right panel).

Discussion

Adaptive responses to oxidative environment are essential to cancer cell survival and therefore tumor progression [10]. Here, we show that the MK2 signaling pathway allows these adaptive responses in liver cancer. First, we found that MK2 and its substrate Hsp27 level is up-regulated in human liver tumors. Furthermore, MK2/Hsp27 signaling pathway is activated by oxidative stress, i.e. H_2O_2, in HCC and CCA cancer cells. MK2 inhibition makes liver cancer cells more sensitive to H_2O_2-induced oxidative stress by abrogating antioxidant defenses and cytoprotective HB-EGF/EGFR signaling. The scaffold protein EBP50, a protein expressed in liver epithelia and overexpressed in liver cancers, regulates MK2 signaling towards Hsp27.

The heat shock protein Hsp27 has been identified as the major substrate of MK2 [23]. We found that H_2O_2 was a potent activator of MK2 responsible for the phosphorylation of Hsp27 in liver cancer cells. Because Hsp27 displays anti-apoptotic properties [24], it may contribute to the anti-apoptotic effect of MK2 in liver cancer cells subjected to oxidative stress. We showed that Hsp27 downregulation by siRNA sensitizes cells to H_2O_2-induced apoptosis, strengthening the anti-apoptotic role of Hsp27 in liver cancer cells, as previously suggested in colon cancer stem cells [41]. In neutrophils, anti-apoptotic function of Hsp27 is mediated by Akt, which is another substrate of MK2 [25]. In these cells, Hsp27 regulates Akt activation and apoptosis by mediating the interaction between Akt and MK2 [42]. We also observed an MK2-dependent activation of Akt in liver cancer cells exposed to H_2O_2 (data not shown). Recently, a regulation of the MK2-Hsp27-Akt signaling cascade by the Rit GTPases has been highlighted as mediating anti-apoptotic pathway [21]. Here, we propose an anti-apoptotic role for MK2 that is mediated by Hsp27 in liver cancer cells upon oxidative stress.

ACCEPTED MANUSCRIPT

MK2-mediated resistance to oxidative stress in liver cancer

Overall cell survival can be driven by antioxidants that support the excess of ROS in order to maintain cell integrity and genomics. Expression of antioxidants is ensured mainly by the Nrf2 transcription factor. Under basal conditions, Nrf2 is repressed in the cytoplasm by Keap1, which facilitates its ubiquitination and degradation. Upon oxidative stress, Keap1 is released from Nrf2 allowing Nrf2 translocation into the nucleus [36]. In the nucleus, Nrf2 induces the expression of genes such as HO-1 involved in redox homeostasis restoration. Here, we showed that MK2/Hsp27 inhibition prevented the nuclear expression of Nrf2 and decreased the expression of HO-1 induced by oxidative stress in liver cancer cells. HO-1 downregulation has been shown to cause liver cancer cell apoptosis suggesting an anti-apoptotic role of HO-1 [43]. Otherwise, liver content of the antioxidant molecule glutathione is reduced in MK2 knockout mice compared to control mice [44]. Our data provide first evidence for a regulation of Nrf2 responsible for the antioxidant response by MK2/Hsp27 pathway in liver cancer cells. An augmentation of DNA breaks observed could be explained by antioxidant response failure after MK2/Hsp27 pathway inhibition in these cells. MK2/Hsp27 pathway allows then an oxidative stress tolerance through activation of antioxidant response and retention of DNA integrity.

Previous investigations have demonstrated that ROS interfere with the EGFR pathway. H_2O_2 has been shown to regulate EGFR by inducing its phosphorylation [37, 38, 45]. We showed that EGFR activation by H_2O_2 depends on the MK2/Hsp27 pathway in liver cancer cells. Besides to EGFR regulation, it has been shown that H_2O_2 increased EGFR ligand synthesis including amphiregulin and HB-EGF in gastric epithelial cells [37], in bladder and lung carcinoma cell lines [38]. In the latter study, the molecular mechanism underlying HB-EGF upregulation relied on increased activity of the metalloprotease TACE, leading to the ectodomain shedding of proHB-EGF into HB-EGF and the subsequent activation of EGFR [38]. It was demonstrated in

18

monocytes that MK2 activity is necessary for ROS-stimulated TACE activation [46]. Here, we showed that H_2O_2-induced HB-EGF expression depends on MK2 and Hsp27. We cannot exclude a regulation of HB-EGF mRNA by TTP, another MK2 substrate. TTP destabilizes mRNA *via* its binding to AU-rich mRNA elements and is inactivated by phosphorylation [47]. Regarding Hsp27, it has recently been described as a regulator of the stability of mRNAs containing AREs [48]. Using the database "AREsite" [49], we found ARE presence in the 3'UTR of HB-EGF mRNA. Therefore, increased HB-EGF expression could be explained by TTP inactivation and/or by the increased ability of Hsp27 to stabilize HB-EGF mRNA. Furthermore, we demonstrated that the HB-EGF/EGFR signaling module activates the MK2/Hsp27 pathway, suggesting the existence of a positive feedback loop. Interestingly, EGFR has been also shown to regulate the antioxidant transcriptional factor Nrf2 by increasing its activity in lung cancer cells. In these cells, EGFR/Nrf2 favors cell proliferation, tumor progression and resistance to chemotherapies [50-52]. Our data showed that MK2 is involved in EGFR activation and regulates Nrf2 in a positive way. Therefore, we can assume that EGFR is also functionally linked to Nrf2 in liver cancer cells subjected to oxidative stress.

Scaffold proteins containing PDZ domains organize signaling complexes [53]. We herein identified a new regulation of MK2 signaling pathway by the scaffold PDZ protein EBP50. In HCC and CCA liver tumors, an upregulation of EBP50 expression has been reported [54, 55] and suggested to participate in carcinogenesis by regulating β-catenin [56] and EGFR pathways [57]. Previous works performed by our team and others have shown that EBP50 regulates kinases including the receptor tyrosine kinases EGFR [57, 58] and PDGFR [59], and the intracellular kinases Akt [40] and PKCζ. [60]. EBP50 appeared to facilitate phosphorylation of Hsp27 by MK2 in liver cancer cells exposed to oxidative stress. Downregulation of EBP50 in

these cells increased apoptosis. Therefore, we provide evidence for a new regulatory mechanism of MK2 signaling and highlight a novel function of EBP50 in liver biology.

In human liver samples, we found a higher expression of MK2 and Hsp27 in HCC tumors compared with adjacent noncancerous tissues and a combined deregulation of both proteins. MK2 and Hsp27 protein expression was also higher in HCC tumors. Interestingly, MK2 protein expression level has been correlated with MK2 kinase activity in breast cancer [33]. Augmentation of Hsp27 level has been observed both in serum [61] and liver tumor tissue [62, 63] from patients with HCC and also in tumor and bile from patients with CCA [64]. Increased MK2 and Hsp27 expression in liver cancer tissues may be linked to a higher activity of MK2/Hsp27 signaling pathway.

In summary, we have demonstrated that MK2-dependent signaling pathway confers to liver cancer cells ability to survive in oxidative environment through antioxidant defenses and HB-EGF/EGFR pathway activation. MK2 signaling module including Hsp27 and EBP50 in stressed liver cancer cells provides a possible mechanism whereby liver tumors progress under oxidative stress. These data underscore the potential of MK2 as a therapeutic target in liver cancers.

Conflict of interest

The authors declare no conflict of interest.

Acknowledgments

REFRENCES

[1]   Razumilava, N.; Gores, G. J. Cholangiocarcinoma. Lancet 21**:**2168-2179; 2014.

[2]   Bruix, J.; Gores, G. J.; Mazzaferro, V. Hepatocellular carcinoma: clinical frontiers and perspectives. Gut 63**:**844-855; 2014.

[3]   Yu, J.; Shen, J.; Sun, T. T.; Zhang, X.; Wong, N. Obesity, insulin resistance, NASH and hepatocellular carcinoma. Semin. Cancer Biol. 23**:**483-491; 2013.

[4]   Ha, H. L.; Shin, H. J.; Feitelson, M. A.; Yu, D. Y. Oxidative stress and antioxidants in hepatic pathogenesis. World J. Gastroenterol. 16**:**6035-6043; 2010.

[5]   Paracha, U. Z.; Fatima, K.; Alqahtani, M.; Chaudhary, A.; Abuzenadah, A.; Damanhouri, G.; Qadri, I. Oxidative stress and hepatitis C virus. Virol. J. 10**:**251; 2013.

[6]   Marra, M.; Sordelli, I. M.; Lombardi, A.; Lamberti, M.; Tarantino, L.; Giudice, A.; Stiuso, P.; Abbruzzese, A.; Sperlongano, R.; Accardo, M.; Agresti, M.; Caraglia, M.; Sperlongano, P. Molecular targets and oxidative stress biomarkers in hepatocellular carcinoma: an overview. J. Transl. Med. 9**:**171; 2011.

[7]   Reuter, S.; Gupta, S. C.; Chaturvedi, M. M.; Aggarwal, B. B. Oxidative stress, inflammation, and cancer: how are they linked? Free Radic. Biol. Med. 49**:**1603-1616; 2010.

[8]   Tien Kuo, M.; Savaraj, N. Roles of reactive oxygen species in hepatocarcinogenesis and drug resistance gene expression in liver cancers. Mol. Carcinog. 45**:**701-709; 2006.

[9]   Valgimigli, M.; Valgimigli, L.; Trere, D.; Gaiani, S.; Pedulli, G. F.; Gramantieri, L.; Bolondi, L. Oxidative stress EPR measurement in human liver by radical-probe technique. Correlation with etiology, histology and cell proliferation. Free Radic. Res. 36**:**939-948; 2002.

[10]   Costa, A.; Scholer-Dahirel, A.; Mechta-Grigoriou, F. The role of reactive oxygen species and metabolism on cancer cells and their microenvironment. Semin. Cancer Biol. 25**:**23-32; 2014.

[11]   Gutierrez-Uzquiza, A.; Arechederra, M.; Bragado, P.; Aguirre-Ghiso, J. A.; Porras, A. p38alpha mediates cell survival in response to oxidative stress via induction of antioxidant genes: effect on the p70S6K pathway. J. Biol. Chem. 287**:**2632-2642; 2012.

[12]   Shaw, M.; Cohen, P.; Alessi, D. R. The activation of protein kinase B by H2O2 or heat shock is mediated by phosphoinositide 3-kinase and not by mitogen-activated protein kinase-activated protein kinase-2. Biochem. J. 336 (Pt 1)**:**241-246; 1998.

[13]   Tran, H.; Maurer, F.; Nagamine, Y. Stabilization of urokinase and urokinase receptor mRNAs by HuR is linked to its cytoplasmic accumulation induced by activated mitogen-activated protein kinase-activated protein kinase 2. Mol. Cell Biol. 23**:**7177-7188; 2003.

[14]   Stokoe, D.; Campbell, D. G.; Nakielny, S.; Hidaka, H.; Leevers, S. J.; Marshall, C.; Cohen, P. MAPKAP kinase-2; a novel protein kinase activated by mitogen-activated protein kinase. Embo J. 11**:**3985-3994; 1992.

[15]   Rouse, J.; Cohen, P.; Trigon, S.; Morange, M.; Alonso-Llamazares, A.; Zamanillo, D.; Hunt, T.; Nebreda, A. R. A novel kinase cascade triggered by stress and heat shock that stimulates MAPKAP kinase-2 and phosphorylation of the small heat shock proteins. Cell 78**:**1027-1037; 1994.

[16]   Kotlyarov, A.; Neininger, A.; Schubert, C.; Eckert, R.; Birchmeier, C.; Volk, H. D.; Gaestel, M. MAPKAP kinase 2 is essential for LPS-induced TNF-alpha biosynthesis. Nat. Cell Biol. 1**:**94-97; 1999.

[17]   Moretto, N.; Bertolini, S.; Iadicicco, C.; Marchini, G.; Kaur, M.; Volpi, G.; Patacchini, R.; Singh, D.; Facchinetti, F. Cigarette smoke and its component acrolein augment IL-8/CXCL8 mRNA stability via p38 MAPK/MK2 signaling in human pulmonary cells. Am. J. Physiol. Lung cell. Mol. Physiol. 303**:**L929-938; 2012.

[18]   Reinhardt, H. C.; Yaffe, M. B. Kinases that control the cell cycle in response to DNA damage: Chk1, Chk2, and MK2. Curr. Opin. Cell Biol. 21**:**245-255; 2009.

[19]   Johansen, C.; Vestergaard, C.; Kragballe, K.; Kollias, G.; Gaestel, M.; Iversen, L. MK2 regulates the early stages of skin tumor promotion. Carcinogenesis 30**:**2100-2108; 2009.

[20]   Reinhardt, H. C.; Aslanian, A. S.; Lees, J. A.; Yaffe, M. B. p53-deficient cells rely on ATM- and ATR-mediated checkpoint signaling through the p38MAPK/MK2 pathway for survival after DNA damage. Cancer Cell 11**:**175-189; 2007.

[21]   Cai, W.; Rudolph, J. L.; Harrison, S. M.; Jin, L.; Frantz, A. L.; Harrison, D. A.; Andres, D. A. An evolutionarily conserved Rit GTPase-p38 MAPK signaling pathway mediates oxidative stress resistance. Mol. Biol. Cell 22**:**3231-3241; 2011.

[22]   Tian, L.; Chen, J.; Chen, M.; Gui, C.; Zhong, C. Q.; Hong, L.; Xie, C.; Wu, X.; Yang, L.; Ahmad, V.; Han, J. The p38 pathway regulates oxidative stress tolerance by phosphorylation of mitochondrial protein IscU. J Biol Chem 289**:**31856-31865; 2014.

[23]   Stokoe, D.; Engel, K.; Campbell, D. G.; Cohen, P.; Gaestel, M. Identification of MAPKAP kinase 2 as a major enzyme responsible for the phosphorylation of the small mammalian heat shock proteins. FEBS Lett. 313**:**307-313; 1992.

[24]   Kostenko, S.; Moens, U. Heat shock protein 27 phosphorylation: kinases, phosphatases, functions and pathology. Cell. Mol. Life Sci. 66**:**3289-3307; 2009.

[25]   Rane, M. J.; Pan, Y.; Singh, S.; Powell, D. W.; Wu, R.; Cummins, T.; Chen, Q.; McLeish, K. R.; Klein, J. B. Heat shock protein 27 controls apoptosis by regulating Akt activation. J. Biol. Chem. 278**:**27828-27835; 2003.

[26]   Alford, K. A.; Glennie, S.; Turrell, B. R.; Rawlinson, L.; Saklatvala, J.; Dean, J. L. Heat shock protein 27 functions in inflammatory gene expression and transforming growth factor-beta-activated kinase-1 (TAK1)-mediated signaling. J. Biol. Chem. 282**:**6232-6241; 2007.

[27]   Waugh, D. J.; Wilson, C. The interleukin-8 pathway in cancer. Clin. Cancer Res. 14**:**6735-6741; 2008.

[28]   Rane, M. J.; Coxon, P. Y.; Powell, D. W.; Webster, R.; Klein, J. B.; Pierce, W.; Ping, P.; McLeish, K. R. p38 Kinase-dependent MAPKAPK-2 activation functions as 3-phosphoinositide-dependent kinase-2 for Akt in human neutrophils. J. Biol. Chem. 276**:**3517-3523; 2001.

[29]   Weber, H. O.; Ludwig, R. L.; Morrison, D.; Kotlyarov, A.; Gaestel, M.; Vousden, K. H. HDM2 phosphorylation by MAPKAP kinase 2. Oncogene 24**:**1965-1972; 2005.

[30]   Felix, R. S.; Colleoni, G. W.; Caballero, O. L.; Yamamoto, M.; Almeida, M. S.; Andrade, V. C.; Chauffaille Mde, L.; Silva, W. A., Jr.; Begnami, M. D.; Soares, F. A.; Simpson, A. J.; Zago, M. A.; Vettore, A. L. SAGE analysis highlights the importance of p53csv, ddx5, mapkapk2 and ranbp2 to multiple myeloma tumorigenesis. Cancer Lett. 278**:**41-48; 2009.

[31]   Liu, B.; Yang, L.; Huang, B.; Cheng, M.; Wang, H.; Li, Y.; Huang, D.; Zheng, J.; Li, Q.; Zhang, X.; Ji, W.; Zhou, Y.; Lu, J. A functional copy-number variation in MAPKAPK2 predicts risk and prognosis of lung cancer. Am. J. Hum. Genet. 91**:**384-390; 2012.

[32]   Birner, P.; Beer, A.; Vinatzer, U.; Stary, S.; Hoftberger, R.; Nirtl, N.; Wrba, F.; Streubel, B.; Schoppmann, S. F. MAPKAP kinase 2 overexpression influences prognosis in gastrointestinal stromal tumors and associates with copy number variations on chromosome 1 and expression of p38 MAP kinase and ETV1. Clin. Cancer Res. 18**:**1879-1887; 2012.

[33]   Salh, B.; Marotta, A.; Wagey, R.; Sayed, M.; Pelech, S. Dysregulation of phosphatidylinositol 3-kinase and downstream effectors in human breast cancer. Int. J. Cancer 98**:**148-154; 2002.

[34]   Fouassier, L.; Yun, C. C.; Fitz, J. G.; Doctor, R. B. Evidence for ezrin-radixin-moesin-binding phosphoprotein 50 (EBP50) self-association through PDZ-PDZ interactions. J. Biol. Chem. 275**:**25039-25045.; 2000.

[35]   Anderson, D. R.; Meyers, M. J.; Vernier, W. F.; Mahoney, M. W.; Kurumbail, R. G.; Caspers, N.; Poda, G. I.; Schindler, J. F.; Reitz, D. B.; Mourey, R. J. Pyrrolopyridine inhibitors of mitogen-activated protein kinase-activated protein kinase 2 (MK-2). J. Med. Chem. 50**:**2647-2654; 2007.

[36]   Shelton, P.; Jaiswal, A. K. The transcription factor NF-E2-related factor 2 (Nrf2): a protooncogene? FASEB J. 27**:**414-423; 2013.

[37]   Miyazaki, Y.; Hiraoka, S.; Tsutsui, S.; Kitamura, S.; Shinomura, Y.; Matsuzawa, Y. Epidermal growth factor receptor mediates stress-induced expression of its ligands in rat gastric epithelial cells. Gastroenterology 120**:**108-116; 2001.

[38]   Fischer, O. M.; Hart, S.; Gschwind, A.; Prenzel, N.; Ullrich, A. Oxidative and osmotic stress signaling in tumor cells is mediated by ADAM proteases and heparin-binding epidermal growth factor. Mol. Cell Biol. 24**:**5172-5183; 2004.

[39]   Rao, G. N. Hydrogen peroxide induces complex formation of SHC-Grb2-SOS with receptor tyrosine kinase and activates Ras and extracellular signal-regulated protein kinases group of mitogen-activated protein kinases. Oncogene 13**:**713-719; 1996.

[40]   Wang, B.; Yang, Y.; Friedman, P. A. Na/H Exchange Regulatory Factor 1, a Novel AKT-associating Protein, Regulates Extracellular Signal-regulated Kinase Signaling through a B-Raf-Mediated Pathway. Mol. Biol. Cell 19**:**1637-1645; 2008.

[41]   Lin, S. P.; Lee, Y. T.; Wang, J. Y.; Miller, S. A.; Chiou, S. H.; Hung, M. C.; Hung, S. C. Survival of cancer stem cells under hypoxia and serum depletion via decrease in PP2A activity and activation of p38-MAPKAPK2-Hsp27. PLoS One 7**:**e49605; 2012.

[42]   Wu, R.; Kausar, H.; Johnson, P.; Montoya-Durango, D. E.; Merchant, M.; Rane, M. J. Hsp27 regulates Akt activation and polymorphonuclear leukocyte apoptosis by scaffolding MK2 to Akt signal complex. J. Biol. Chem. 282**:**21598-21608; 2007.

[43]   Sass, G.; Leukel, P.; Schmitz, V.; Raskopf, E.; Ocker, M.; Neureiter, D.; Meissnitzer, M.; Tasika, E.; Tannapfel, A.; Tiegs, G. Inhibition of heme oxygenase 1 expression by small interfering RNA decreases orthotopic tumor growth in livers of mice. Int J Cancer 123**:**1269-1277; 2008.

[44]   Jackson, R. M.; Gupta, C. Hypoxia and kinase activity regulate lung epithelial cell glutathione. Experimental lung research 36**:**45-56; 2010.

[45]   Gamou, S.; Shimizu, N. Hydrogen peroxide preferentially enhances the tyrosine phosphorylation of epidermal growth factor receptor. FEBS Lett. 357**:**161-164; 1995.

[46]   Scott, A. J.; O'Dea, K. P.; O'Callaghan, D.; Williams, L.; Dokpesi, J. O.; Tatton, L.; Handy, J. M.; Hogg, P. J.; Takata, M. Reactive oxygen species and p38 mitogen-activated protein kinase mediate tumor necrosis factor alpha-converting enzyme (TACE/ADAM-17) activation in primary human monocytes. J. Biol. Chem. 286**:**35466-35476; 2011.

[47]   Ronkina, N.; Menon, M. B.; Schwermann, J.; Tiedje, C.; Hitti, E.; Kotlyarov, A.; Gaestel, M. MAPKAP kinases MK2 and MK3 in inflammation: complex regulation of TNF biosynthesis via expression and phosphorylation of tristetraprolin. Biochem. Pharmacol. 80**:**1915-1920; 2010.

[48]   Li, M. L.; Defren, J.; Brewer, G. Hsp27 and F-box protein beta-TrCP promote degradation of mRNA decay factor AUF1. Mol. Cell. Biol. 33**:**2315-2326; 2013.

[49]   Gruber, A. R.; Fallmann, J.; Kratochvill, F.; Kovarik, P.; Hofacker, I. L. AREsite: a database for the comprehensive investigation of AU-rich elements. Nucleic Acids Res. 39**:**D66-69; 2011.

[50]   Papaiahgari, S.; Yerrapureddy, A.; Hassoun, P. M.; Garcia, J. G.; Birukov, K. G.; Reddy, S. P. EGFR-activated signaling and actin remodeling regulate cyclic stretch-induced NRF2-ARE activation. American journal of respiratory cell and molecular biology 36**:**304-312; 2007.

[51]   Weaver, Z.; Difilippantonio, S.; Carretero, J.; Martin, P. L.; El Meskini, R.; Iacovelli, A. J.; Gumprecht, M.; Kulaga, A.; Guerin, T.; Schlomer, J.; Baran, M.; Kozlov, S.; McCann, T.; Mena, S.; Al-Shahrour, F.; Alexander, D.; Wong, K. K.; Van Dyke, T. Temporal molecular and biological assessment of an erlotinib-resistant lung adenocarcinoma model reveals markers of tumor progression and treatment response. Cancer Res 72**:**5921-5933; 2012.

[52]   Yamadori, T.; Ishii, Y.; Homma, S.; Morishima, Y.; Kurishima, K.; Itoh, K.; Yamamoto, M.; Minami, Y.; Noguchi, M.; Hizawa, N. Molecular mechanisms for the regulation of Nrf2-mediated cell proliferation in non-small-cell lung cancers. Oncogene 31**:**4768-4777; 2012.

[53]   Zhang, M.; Wang, W. Organization of signaling complexes by PDZ-domain scaffold proteins. Acc. Chem. Res. 36**:**530-538; 2003.

[54]   Fouassier, L.; Duan, C. Y.; Feranchak, A. P.; Yun, C. H.; Sutherland, E.; Simon, F.; Fitz, J. G.; Doctor, R. B. Ezrin-radixin-moesin-binding phosphoprotein 50 is expressed at the apical membrane of rat liver epithelia. Hepatology 33**:**166-176.; 2001.

[55]   Fouassier, L.; Rosenberg, P.; Mergey, M.; Saubamea, B.; Claperon, A.; Kinnman, N.; Chignard, N.; Jacobsson-Ekman, G.; Strandvik, B.; Rey, C.; Barbu, V.; Hultcrantz, R.; Housset, C. Ezrin-radixin-moesin-binding phosphoprotein (EBP50), an estrogen-inducible scaffold protein, contributes to biliary epithelial cell proliferation. Am. J. Pathol. 174**:**869-880; 2009.

[56]   Shibata, T.; Chuma, M.; Kokubu, A.; Sakamoto, M.; Hirohashi, S. EBP50, a beta-catenin-associating protein, enhances Wnt signaling and is over-expressed in hepatocellular carcinoma. Hepatology 38**:**178-186; 2003.

[57]   Claperon, A.; Guedj, N.; Mergey, M.; Vignjevic, D.; Desbois-Mouthon, C.; Boissan, M.; Saubamea, B.; Paradis, V.; Housset, C.; Fouassier, L. Loss of EBP50 stimulates EGFR activity to induce EMT phenotypic features in biliary cancer cells. Oncogene 31**:**1376-1388; 2012.

[58]   Lazar, C. S.; Cresson, C. M.; Lauffenburger, D. A.; Gill, G. N. The Na+/H+ exchanger regulatory factor stabilizes epidermal growth factor receptors at the cell surface. Mol. Biol. Cell 15**:**5470-5480; 2004.

[59]   Maudsley, S.; Zamah, A. M.; Rahman, N.; Blitzer, J. T.; Luttrell, L. M.; Lefkowitz, R. J.; Hall, R. A. Platelet-derived growth factor receptor association with Na(+)/H(+) exchanger regulatory factor potentiates receptor activity. Mol. Cell. Biol. 20**:**8352-8363.; 2000.

[60]   Leslie, K. L.; Song, G. J.; Barrick, S.; Wehbi, V. L.; Vilardaga, J. P.; Bauer, P. M.; Bisello, A. Ezrin-radixin-moesin-binding phosphoprotein 50 (EBP50) and nuclear factor-kappaB (NF-kappaB): a feed-forward loop for systemic and vascular inflammation. J. Biol. Chem. 288**:**36426-36436; 2013.

[61]   Gruden, G.; Carucci, P.; Lolli, V.; Cosso, L.; Dellavalle, E.; Rolle, E.; Cantamessa, A.; Pinach, S.; Abate, M. L.; Campra, D.; Brunello, F.; Bruno, G.; Rizzetto, M.; Perin, P. C. Serum heat shock protein 27 levels in patients with hepatocellular carcinoma. Cell Stress Chaperones 18**:**235-241; 2013.

[62]   Lee, I. N.; Chen, C. H.; Sheu, J. C.; Lee, H. S.; Huang, G. T.; Yu, C. Y.; Lu, F. J.; Chow, L. P. Identification of human hepatocellular carcinoma-related biomarkers by two-dimensional difference gel electrophoresis and mass spectrometry. J. Proteome Res. 4**:**2062-2069; 2005.

[63]   Lim, S. O.; Park, S. G.; Yoo, J. H.; Park, Y. M.; Kim, H. J.; Jang, K. T.; Cho, J. W.; Yoo, B. C.; Jung, G. H.; Park, C. K. Expression of heat shock proteins (HSP27, HSP60, HSP70, HSP90, GRP78, GRP94) in hepatitis B virus-related hepatocellular carcinomas and dysplastic nodules. World J. Gastroenterol. 11**:**2072-2079; 2005.

[64]   Sato, Y.; Harada, K.; Sasaki, M.; Yasaka, T.; Nakanuma, Y. Heat shock proteins 27 and 70 are potential biliary markers for the detection of cholangiocarcinoma. Am. J. Pathol. 180**:**123-130; 2012.

MK2-mediated resistance to oxidative stress in liver cancer

FIGURE LEGENDS

Figure 1 – MK2 and Hsp27 status in liver tumors from human. (A) Real-time PCR analysis of MK2 and Hsp27 mRNA expression and linear regression in 70 human paired HCC (T)/non-tumor (NT) liver tissue samples. (B-C) Representative immunostaining showing MK2 and Hsp27 expression in a HCC tumor compared to paired non-tumor tissue (n=7) (B) and in CCA tumor (n=10) compared to adjacent non-tumor liver (C). Statistical analysis: T *vs* NT: Wilcoxon test for paired values. ***, $P < 0.001$. Original magnification: x200.

Figure 2 – Oxidative stress triggered by H_2O_2 activates MK2 pathway in liver cancer cells. (A) HCC (PLC/PRF/5, HepG2) and CCA (Mz-ChA-1, TFK-1) cells were incubated with H_2O_2 (0.5 mM) in the presence or absence of MK2i (5 μM) for various times; the phosphorylation status of MK2 and Hsp27 was examined by western blot. MK2 was visualized using a specific antibody that recognizes MK2 irrespective of its phosphorylation status; MK2 phosphorylation was attested by an upper shift in electrophoretic mobility. (B) MK2 downregulation was achieved by siRNA. HCC (PLC/PRF/5) and CCA (Mz-ChA-1) cells were transiently transfected with MK2 or Ctrl siRNA for 48 h and incubated with H_2O_2 for 30 min. Representative blots of at least four experiments are shown. (C) HCC (PLC/PRF/5) and CCA (Mz-ChA-1) cells were incubated with increasing doses of H_2O_2 for 48 h in the presence or absence of MK2i. Cell viability was measured using MTT assay. Statistical analysis: n=6 in duplicate; Mann-Whitney; ** $P < 0.01$, *** $P < 0.001$, *vs* no H_2O_2. # $P < 0.05$, ## $P < 0.01$, ### $P < 0.001$ *vs* H_2O_2 without MK2i.

Figure 3 – Inhibition of MK2 decreases liver cancer cells ability to survive in oxidative environment. (A-C) Apoptosis analysis by caspase-3 and PARP cleavage. (A) Cells were treated with 0.5 mM of H_2O_2 for 24 h in the presence or absence of MK2i; (B-C) Cells were transiently

transfected with MK2 (B), Hsp27 (C) or Ctrl siRNA (B-C) for 48 h and incubated with H_2O_2 for 24 h. Representative images of four independent experiments are shown.

Figure 4 – Inhibition of MK2 prevents oxidative stress-induced DNA breaks. (A-C) HCC (PLC/PRF/5) and CCA (Mz-ChA-1) cells were treated with H_2O_2 for 24 h in the presence or absence of MK2i. γH2AX nuclear localization and protein expression were evaluated by immunofluorescence (A) and the number of γH2AX-positive cells (B), and by western blot (C). (D) Hsp27 was inhibited by siRNA. HCC (PLC/PRF/5) and CCA (Mz-ChA-1) cells were transiently transfected with Hsp27 or Ctrl siRNA for 48 h and incubated with H_2O_2 for 24 h. Original magnification: x63. Protein level of γH2AX was evaluated by western blot. Statistical analysis: n=4; Student's t-test; * $P < 0.05$ *vs* Ctrl, [#] $P < 0.05$ *vs* H_2O_2.

Figure 5 − Inhibition of MK2 prevents the nuclear localization of Nrf2 and expression of HO-1, increases ROS production and DNA breaks. (A-B) HCC (PLC/PRF/5) and CCA (Mz-ChA-1) cells were treated with H_2O_2 for 4 h (A) or 8 h (B) in the presence or absence of MK2i. (A) Subcellular localization of Nrf2 was analyzed by immunofluorescence; (B) HO-1 expression was analyzed by western blot. (C-D) HCC (PLC/PRF/5) and CCA (Mz-ChA-1) cells were transiently transfected with Nrf2 or Ctrl siRNA for 48 h and incubated with H_2O_2 for 6 h (C) or 24 h (D). HO-1 and γH2AX expression was analyzed by western blot. (E) ROS level was detected by dihydroethidium (DHE) fluorescent probe assay. HCC (PLC/PRF/5) and CCA (Mz-ChA-1) cells were treated with H_2O_2 for 24 h in the presence or absence of MK2i. (F) HCC (PLC/PRF/5) and CCA (Mz-ChA-1) cells were transiently transfected with Hsp27 or Ctrl siRNA for 48 h and incubated with H_2O_2 for 6 h. Original magnification: x63. Statistical analysis: n=4; Student's t-test; [#] $P < 0.05$ *vs* H_2O_2.

Figure 6 − Inhibition of MK2 abrogates H_2O_2-induced activation of HB-EGF/EGFR pathway in liver cancer cells. (A-E) EGFR activation and HB-EGF expression in response to H_2O_2 was analyzed either by western blot (A, B, E) or by RT-qPCR (C and D). HCC (PLC/PRF/5) and CCA (Mz-ChA-1) cells were serum-deprived for 24 h (A-B) or not (C and D) and treated with H_2O_2 for 1 h (A-B) or 5 h (C) in the presence or absence of MK2i; (D) Cells were transiently transfected with Hsp27 or Ctrl siRNA for 67 h and treated with H_2O_2 for 5 h; (E) Western blot analysis of the cellular content of HB-EGF. (F) Activation of MK2 pathway by HB-EGF. Cells were serum-deprived for 24 h and pretreated with or without MK2i 1 h prior to incubation with HB-EGF (50 ng/mL) for 30 min. Statistical analysis: n = 6 in duplicate; Wilcoxon rank-signed test; ** $P < 0.01$ *vs* Ctrl or siCtrl; Mann-Whitney; [#] $P < 0.05$ *vs* H_2O_2.

Figure 7 – Regulation of MK2 pathway by the scaffold protein EBP50. (A) MK2 protein owns a typical PDZ motif at its COOH-tail, LTRL. (B-C) MK2 interacts with EBP50. GST pull-down analysis was performed by incubating immobilized GST recombinant proteins of EBP50 (left panel and middle panel) with Hela cell lysate (right panel); (B) Staining of GST recombinant proteins of EBP50 with Ponceau S (middle panel) and western blot analysis using MK2 and Akt antibodies (right panel); (C) MK2 (left panel) or EBP50 (right panel) was immunoprecipitated with specific antibody or control immunoglobulin G from whole-cell lysates of Mz-ChA-1 cells. Western blotting was performed with an antibody against EBP50 (left panel) or MK2 (right panel). (D) Loss of EBP50 decreases MK2-dependent cell signaling. HCC (PLC/PRF/5) and CCA (Mz-ChA-1) cells were transiently transfected with EBP50 or Ctrl siRNA for 72 h and treated or not with H_2O_2. Phosphorylation status of MK2 and Hsp27 was analyzed by western blotting. (E) H_2O_2 promotes interaction between EBP50 and Hsp27. Mz-ChA-1 cells were treated or not with 500 μM of H_2O_2 for 30 min. Cell lysate was incubated with 25 μg of GST

only or GST-EBP50 for 2 h and Hsp27 was detected by western blotting. (F-G) Loss of EBP50 causes apoptosis and DNA breaks. HCC (PLC/PRF/5) and CCA (Mz-ChA-1) cells were transiently transfected with EBP50 or Ctrl siRNA for 48 h and treated or not with H_2O_2 for 24 h. Western blotting was performed to analyze caspase-3 and PARP cleavage (F) and γH2AX expression (G). Representative images of four independent experiments are shown.

Figure 8 – EBP50 status in liver tumors from human. (A-B) Real-time PCR analysis of EBP50 mRNA expression (A) and linear regression (B) in 70 human paired HCC (T)/nontumor (NT) liver tissue samples. (C) Representative immunostaining showing EBP50 expression in a HCC tumor compared to paired nontumor tissue (n=7) and in CCA tumor (n=10) compared to adjacent nontumor liver. Statistical analysis: T *vs* NT: Wilcoxon test for paired values. ***, $P < 0.001$. Original magnification: x200.

Highlights

- MK2 and Hsp27 are overexpressed in human primary liver cancer

- MK2/Hsp27 promotes liver cancer cell survival in an oxidative environment

- MK2/Hsp27 regulates Nrf2/HO-1 and HB-EGF/EGFR survival pathways

- The scaffold protein EBP50 is an MK2 partner, promoting MK2-dependent signaling

Table 1: Clinical and pathological characteristics of patients with HCC (n=70) and CCA (n=10)

HCC

Age (years)	
Mean (± SD)	62 (± 13)
Sex ratio (M/F)	5.4 (59/11)
Etiology of chronic liver disease, n	
HCV infection	14 (20 %)
HBV infection	20 (29 %)
Alcohol abuse	4 (6 %)
Hemochromatosis	2 (3 %)
NASH	9 (13%)
Combined viral hepatitis and alcohol	7 (10 %)
Combined metabolic syndrome and alcohol	6 (9 %)
Undetermined	8 (11 %)
Cirrhosis, n (%)	33 (47 %)
Tumor size (mm)	
Mean (± SD)	63.1 (± 48.8)
Number of tumors, n	
Single	55 (77 %)
Multiple	15 (23 %)
Tumor grade, n *	
Well differentiated	11 (16%)
Moderately differentiated	35 (51 %)
Poorly differentiated	23 (33 %)
Invasion	14 (20 %)

* n=69 available

CCA

Age (years)	
Mean (± SD)	67.5 (±3.9)
Sex ratio (M/F)	1 (5/5)
Tumor size (mm)	
Mean (± SD)	(75.5±16)
Tumor grade	
Well differentiated	3 (30%)
Moderately differentiated	6 (60%)
Poorly differentiated	1 (10%)
pTNM (7th edition)	
T1	3 (30%)
T2a	1 (10%)
T2b	6 (60%)
Vascular invasion	6 (60%)
Perineural invasion	2 (20%)
Lymph node metastasis	1 (10%)

Table 2: Primary antibodies used for immunodetection

Name	Species	Manufacturer	Clone	Dilution	Antigen unmasking
Akt	Rabbit	Cell Signaling	C67E7	1/1000 (WB)	
Caspase-3	Rabbit	Cell Signaling		1/500 (WB)	
EBP50	Rabbit	Pierce		1/1000 (WB), 1/200 (IHC & IP)	Citrate, pH 6 (15 min 95°C)
EGFR	Rabbit	Santa Cruz		1/250 (WB)	
p-Y1068 EGFR	Rabbit	Cell Signaling		1/1000 (WB)	
GAPDH	Mouse	Santa Cruz	6C5	1/5000 (WB)	
HB-EGF	Mouse	Santa Cruz	G-11	1/250 (WB)	
HO-1	Mouse	Pierce	HO-1-1	1/1000 (WB)	
Hsp27	Rabbit	Enzo		1/1000 (WB)	
Hsp27	Mouse	Enzo	G3.1	1/200 (IHC)	Citrate, pH 6 (15 min 95°C)
p-S78-Hsp27	Rabbit	Cell Signaling		1/1000 (WB)	
MK2	Rabbit	Cell Signaling		1/1000 (WB & IP)	
MK2	Mouse	Santa Cruz	H-66	1/50 (IHC)	EDTA, pH 9 (15 min 95°C)
Nrf2	Rabbit	Santa Cruz	C-20	1/200 (IF)	
Nrf2	Rabbit	Abcam	EP1808Y	1/1000 (WB)	
PARP	Rabbit	Cell Signaling	H-250	1/1000 (WB)	
γH2AX	Mouse	Millipore	JBW301	1/1000 (WB) 1/500 (IF)	

WB, western blot; IHC, immunohistochemistry; IP, immunoprecipitation; IF, immunofluorescence.

Table 3: Primers used for quantitative real-time PCR

Genes	Forward	Reverse
SLC9A3R1 (EBP50)	5' GGCTGGCAACGAAAATGAGC 3'	5' TGTCGCTGTGCAGGTTGAAG 3'
HBEGF	5' GAAAGACTTCCATCTAGTCACAAACA 3'	5' GGGAGGCCCAATCCTAGA 3'
HPRT	5' TAATTGGTGGAGATGATCT 3'	5' TGCCTGACCAAGGAAAGC 3'
HSP27	5' TCCCTGGATGTCAACCACTT 3'	5' GATGTAGCCATGCTCGTCCT 3'
MAPKAPK2	5' GGATGTCAAGCCTGAGAAT 3'	5' CCAGCACTTCTGGAGCCAC 3'

Figure 1

ACCEPTED MANUSCRIPT
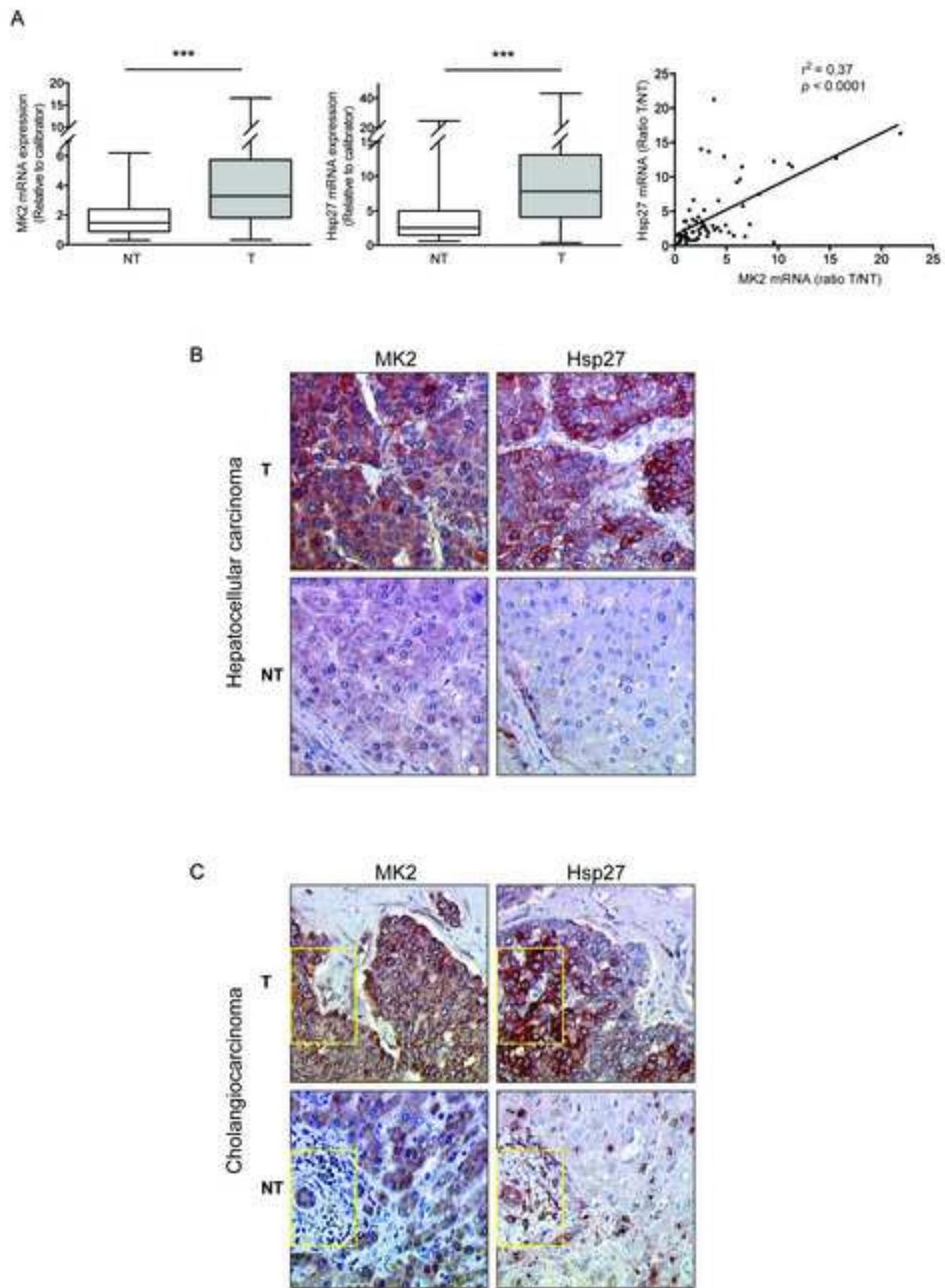
Figure 1
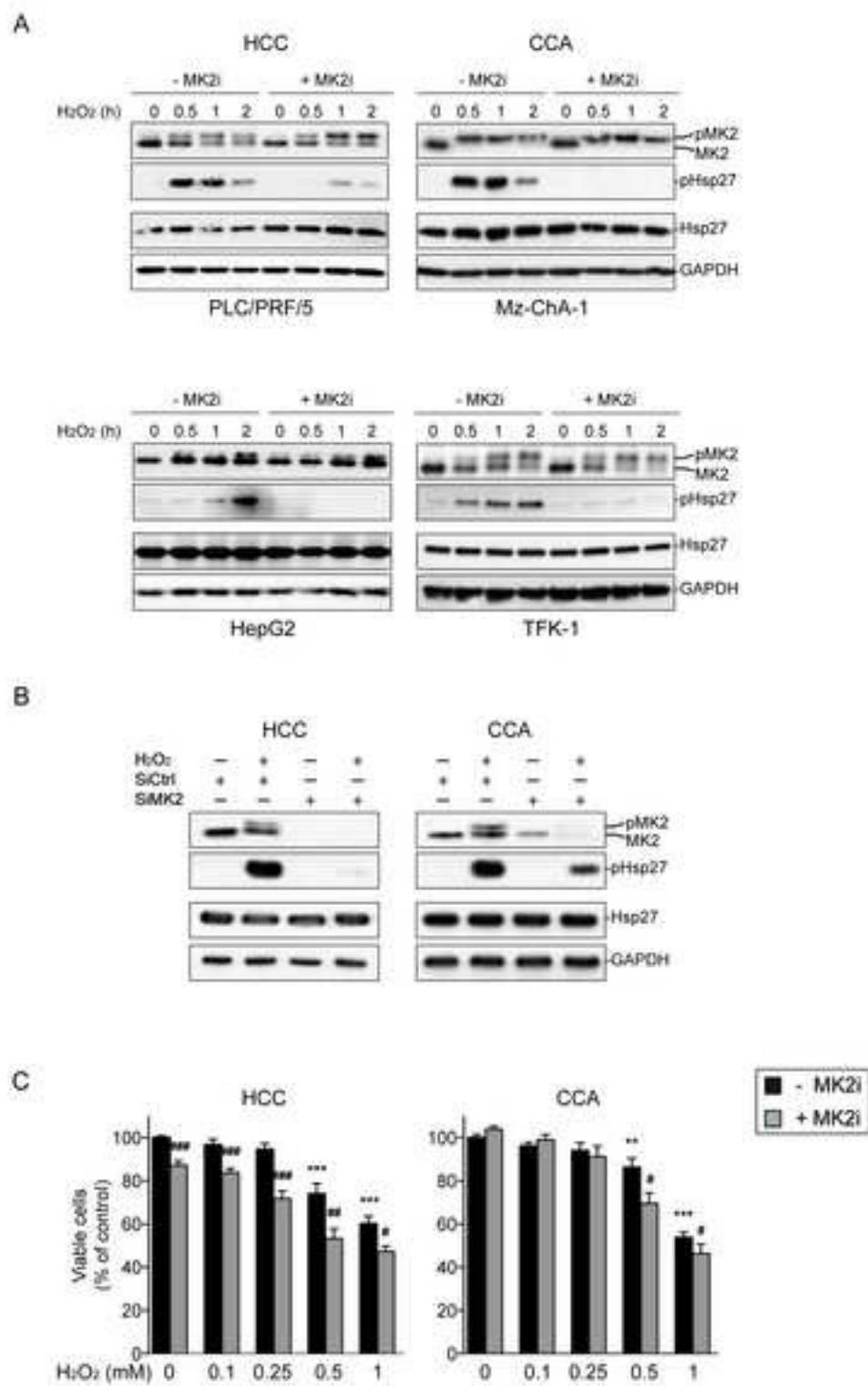
Figure 2
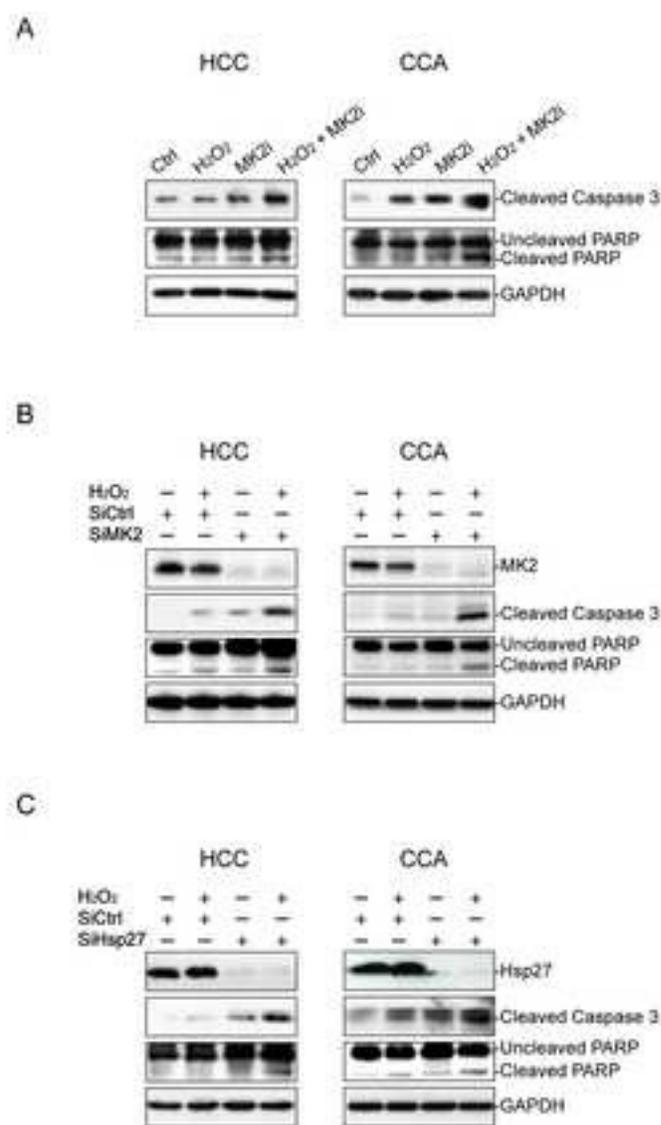
Figure 2

Figure 3
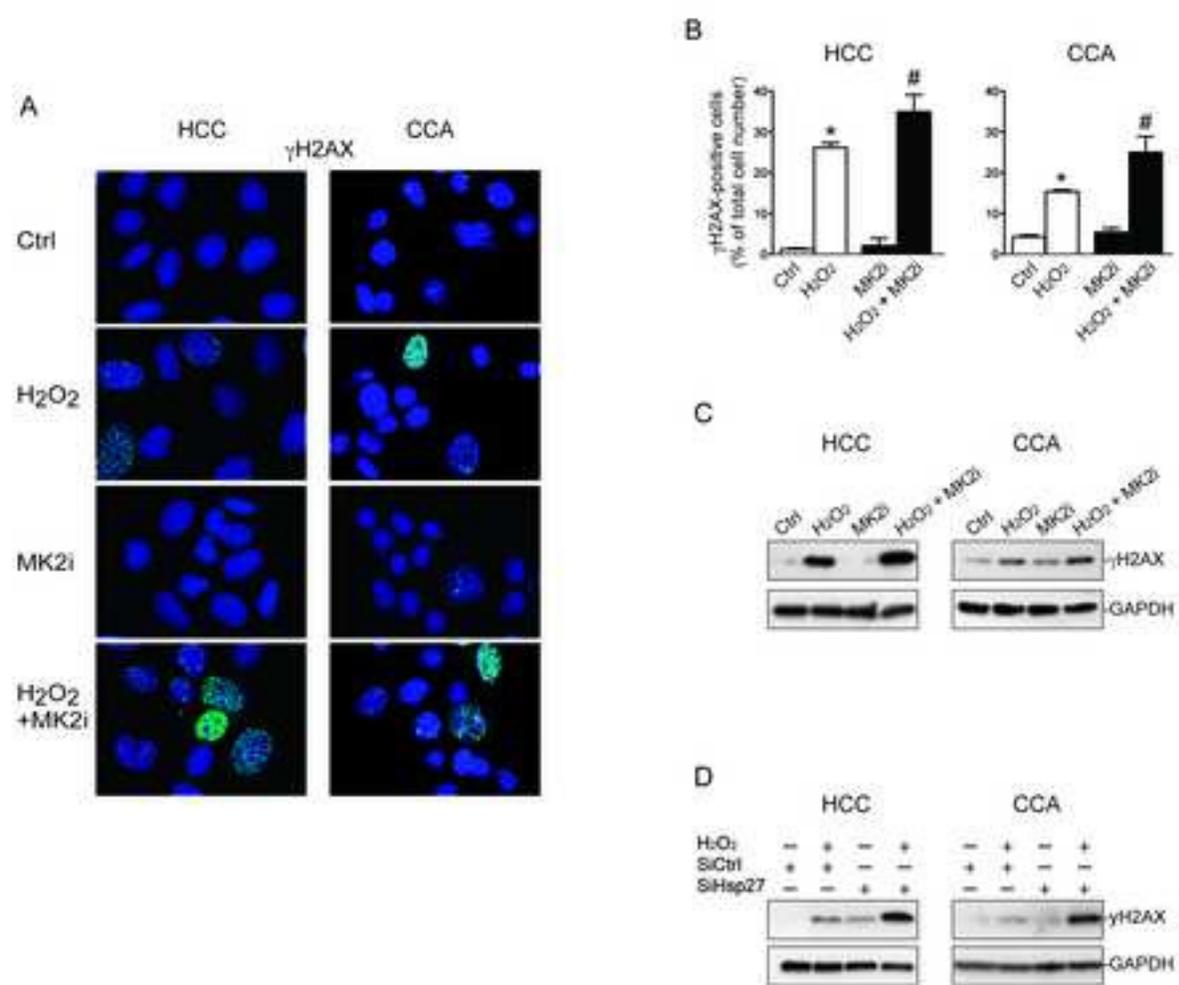
Figure 3

Figure 4

Figure 4

Figure 5

Figure 5

Figure 6

Figure 6

Figure 7

A

| Consensus PDZ motif | X-S/T-X-L |
| MK2 | L-T-R-L |

B

GST-EBP50 wt

GST-EBP50-PDZ1

GST-EBP50-PDZ2

C

WB: EBP50

WB: MK2

D

HCC   CCA

E

F

HCC   CCA

G

HCC   CCA

Figure 7

Figure 8

Figure 8